SI Appendix:

Experimental Methods

1. Synthesis of materials

Synthesis of Ti-Beta

Ti-Beta zeolite has been prepared as follows: 7.503 g of tetraethylammonium hydroxide solution (Sigma-Aldrich, 35 wt% in water) was diluted with 15 g of water. Then, 7.016 g of tetraethylorthosilicate (Sigma-Aldrich, 98 wt%) and 0.201 g of titanium (IV) isopropoxide (Sigma-Aldrich, 97%wt) were added to the solution. The mixture was stirred until complete hydrolysis of the tetraethylorthosilicate and titanium (IV) isopropoxide was obtained. Next, the solution was allowed to reach the desired water ratio by complete evaporation of ethanol, isopropanol, and some water. Finally, 0.670 g of HF solution (Mallinckrodt, 48 wt% in water) was added resulting in a thick gel. The gel composition was SiO_2 / 0.021 TiO_2 / 0.54 TEAOH / 0.53 HF / 6.6 H_2O. This gel was transferred to a Teflon-lined stainless steel autoclave and heated at 140°C for 14 days. The solid was recovered by filtration, extensively washed with water, and dried at 100°C overnight. The solid was calcined at 580ºC for 6 hours to remove the organic content located within the crystalline material.

Synthesis of TS-1

TS-1 zeolite was synthesized following the method reported in the patent literature.(*1*) TS-1 was crystallized from a clear solution prepared by mixing titanium butoxide (TNBT, Sigma-Aldrich 97 wt%), tetraethylorthosilicate (TEOS, Sigma-Aldrich 97 wt%), tetrapropylammonium hydroxide (TPAOH, 1M, Sigma-Aldrich) and deionized water. The mixture was stirred until complete hydrolysis of the tetraethylorthosilicate and titanium butoxide was obtained, then allowing complete evaporation of ethanol, butanol and some water until the desired water ratio was reached. The gel composition was SiO_2 / 0.03 TiO_2 / 0.44 TPAOH / 30 H_2O. The TS-1 reaction mixture was charged into Teflon-lined autoclaves and allowed to crystallize at 175ºC for 5 days. The autoclave was rotated at 50 RPM. After cooling, the solid was recovered by filtration, extensively washed with water, and dried at 100°C overnight. The material was calcined at 580ºC for 6 hours to remove the organic content located within the crystalline material.

Synthesis of Sn-Beta, ^{119}Sn-Beta and CH_3-Sn-Beta

Zeolites were prepared as follows: 7.57 g of tetraethylammonium hydroxide solution (Sigma-Aldrich, 35% (w/w) in water) was diluted with 15 g of water. Next, 7.011 g of tetraethylorthosilicate (Sigma-Aldrich, 98% (w/w)) was added, followed by the addition of 0.121 g of tin (IV) chloride pentahydrate (Sigma-Aldrich, 98% (w/w)), 0.121 ^{119}Sn enriched tin(IV) chloride pentahydrate (Cambridge Isotopes, 82% enrichment) or 0.122 g of methyltin trichloride pentahydrate (Sigma Aldrich, 97 wt%), depending if Sn-Beta, ^{119}Sn-Beta, or CH_3-Sn-Beta were synthesized, respectively. The mixture was stirred until complete hydrolysis of the tetraethylorthosilicate was achieved, and then allowed to reach the desired water ratio by complete evaporation of ethanol and some water. Finally, 0.690 g of HF solution (Mallinckrodt, 48% (w/w) in water) was added, resulting in a thick gel. The gel composition was SiO_2 / 0.01 $SnCl_4$ / 0.55 TEAOH / 0.54 HF / 7.52 H_2O. The

gels were transferred to Teflon-lined stainless steel autoclaves and heated at 140 ^{o}C for 25 days. The solids were recovered by filtration, extensively washed with water, and dried at 373 K overnight. The solids were calcined at 580 ^{o}C for 6 h to remove the organic content located in the crystalline material. X-ray diffraction confirmed that the solid materials have the Beta zeolite topology (see Figure S5 for the diffraction pattern of CH_3-Sn-Beta), and SEM EDS measurements for the Sn-Beta, ^{119}Sn-Beta and CH_3-Sn-Beta samples show a Si:Sn atomic ratio of 125:1, 125:1, and 150:1, respectively.

2. Isomerization reactions

Isomerization experiments were carried out in 10 ml thick-walled glass reactors (VWR) heated in a temperature-controlled oil bath placed on top of a digital stirring hotplate (Fisher Scientific). In a typical experiment, 1.5 g of an aqueous solution composed of 10 wt% glucose and the corresponding catalyst amount to achieve a 1:100 metal:glucose molar ratio were added to the reactor and sealed. The reactor was placed in the oil bath and removed at specific times. The reaction was stopped by cooling the reactor in an ice bath, and small aliquots were taken for analysis. Sample analyses were performed by means of high performance liquid chromatography (HPLC) using an Agilent 1200 system (Agilent Technologies Corp.) equipped with PDA UV (320 nm) and evaporative light-scattering (ELS) detectors. Glucose and fructose concentrations were monitored with a Biorad Aminex HPX87C (300 x 7.8 mm) column (Phenomenex), using ultrapure water (pH = 7) as the mobile phase at a flow rate of 0.60 ml/min and a column temperature of 80 ^{o}C.

3. Adsorption experiments

Sn-BEA or Si-BEA catalyst was mixed with 10 wt% of C13-sugar (glucose or fructose) solution at Sn or Si to sugar (glucose or fructose) molar ratio of 1/100 for two hours at room temperature. The mixture was then centrifuged to separate the solid catalyst from the extra glucose solution. Leftover water was removed by leaving the vessel containing the catalyst open overnight in the hood.

4. Characterization

Powder X-ray diffraction (XRD) patterns were collected by using a Scintag XDS 2000 diffractometer using Cu Kα radiation. Scanning electron microscopy (SEM) with Energy Dispersive X-ray Spectroscopy (EDS) measurements were recorded on a LEO 1550 VP FE SEM at an electron high tension (EHT) of 10 kV. UV-Vis measurements were recorded using a Cary 3G spectrophotometer equipped with a diffuse reflectance cell. IR spectra were recorded on a Nicolet Nexus 470 FTIR using a MCT detector. The samples were pressed pellets of pure powder.

Solid-state, magic angle spinning nuclear magnetic resonance (MAS-NMR) measurements were performed using a Bruker Avance 500MHz spectrometer equipped with a 11.7 T magnet and a Bruker 4mm MAS probe. Samples about 60-80 mg in powder were packed into 4mm ZrO_2 rotors and spun at 14 kHz for MAS

experiments. MAS-NMR experiments were conducted for ^{1}H, ^{13}C, ^{23}Na, and ^{119}Sn nuclei of which operating frequencies are 500.2, 125.5, 132.3, 186.5 MHz, respectively. ^{119}Sn MAS NMR spectra were obtained with a recycle delay time of 2 s or 200 s for dehydrated samples. ^{119}Sn cross polarization (CP) MAS spectra were acquired at spinning rate of 10 kHz and using radio frequency (rf) field strength of 62.6 kHz for contact pulse after 4 μsec-π/2 pulse on the ^{1}H channel and strong ^{1}H decoupling during the acquisition. ^{13}C CPMAS experiments were carried out at similar rf field strength. NMR spectra (in ppm) are reported with referenced to tetramethylsilane (TMS) for ^{1}H and ^{13}C, 1M aqueous solution of $Na(NO_3)_3$ for ^{23}Na, and $(CH_3)_3Sn$ but measured with SnO_2 at -604.3 ppm as a second external reference for ^{119}Sn nuclei. For the determination of the amount of the ring-opened carbonyl carbon, the signal intensity of 214 ppm peak in a ^{13}C MAS spectrum of a fructose/Sn-Beta sample was compared with that of ^{13}C MAS spectrum of a known amount of ^{13}C enriched fructose. Once the nuclear spin number of the carbonyl carbon was determined, the number was compared to the number of Sn sites in the sample. For the calculation of Sn sites, the zeolite was simply considered to be pure SiO_2 and Sn spins were obtained from the Si/Sn ratio. Analogous methods were employed to determine the amount of ring-opened fructose from the glucose/Sn-Beta sample.

UV-Vis measurements were recorded using a Cary 3G spectrophotometer equipped with a diffuse reflectance cell. The results for the Sn-Beta samples show the presence of framework Sn and have been published previously.

Results

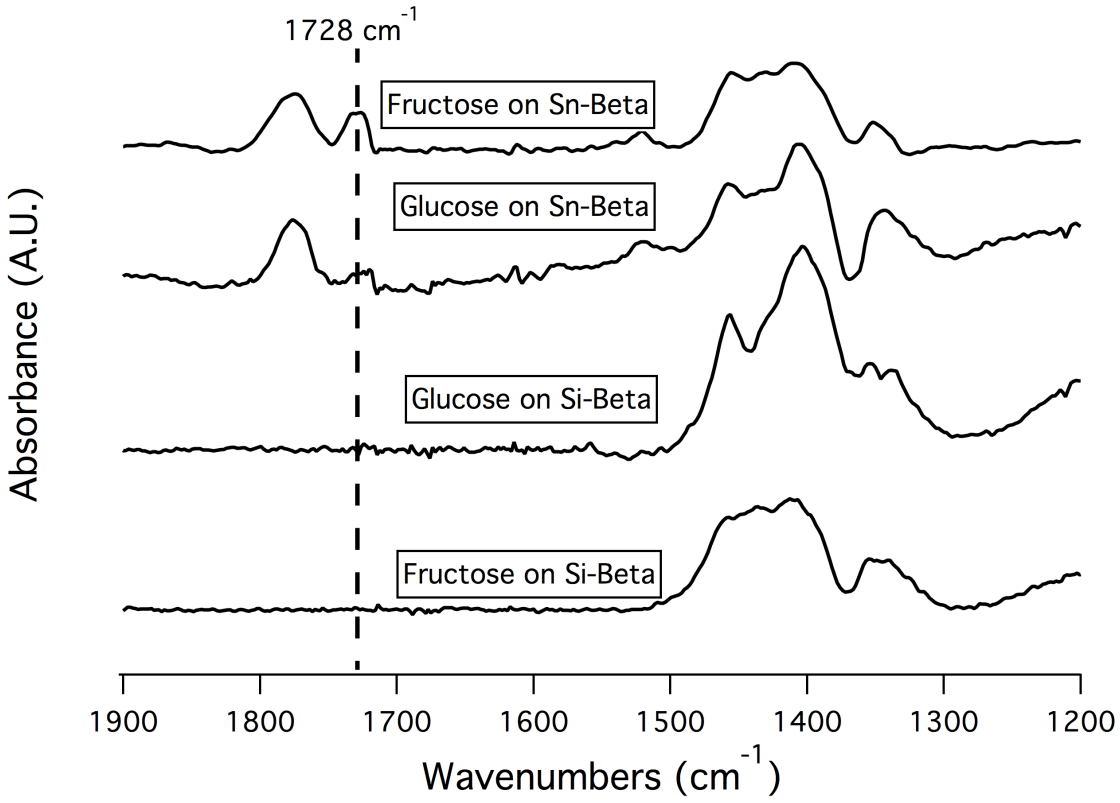

Fig. S1: Infrared spectra of glucose and fructose adsorbed in Sn-Beta and Si-Beta**.** The band at 1775 cm-1 is not assigned to either the ketone or aldedyde groups of the acyclic fructose and glucose, respectively.

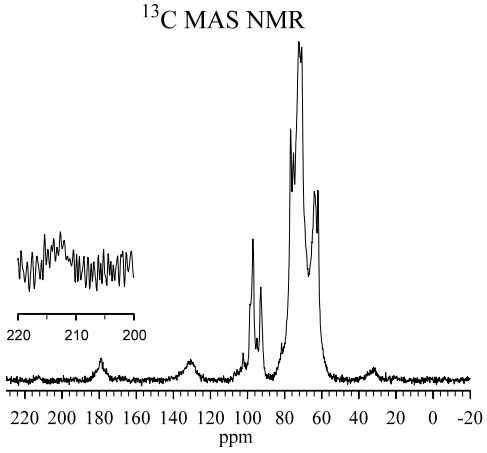

Fig. S2: ^{13}C solid-state NMR spectrum of glucose adsorbed in Sn-Beta.

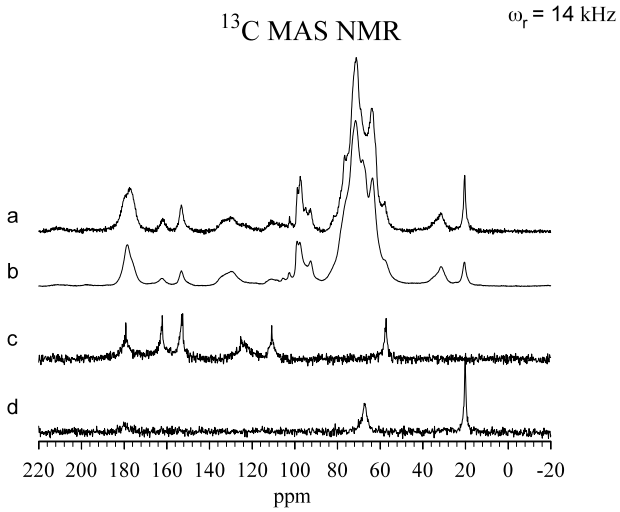

Fig. S3: ^{13}C solid-state NMR of Sn-Beta after reaction conditions using either labeled fructose (a) or labeled glucose (b) as the reactant. Also, HMF absorbed into Sn-Beta (c) and lactic acid absorbed into Si-Beta (d) at room temperature are shown for comparison.

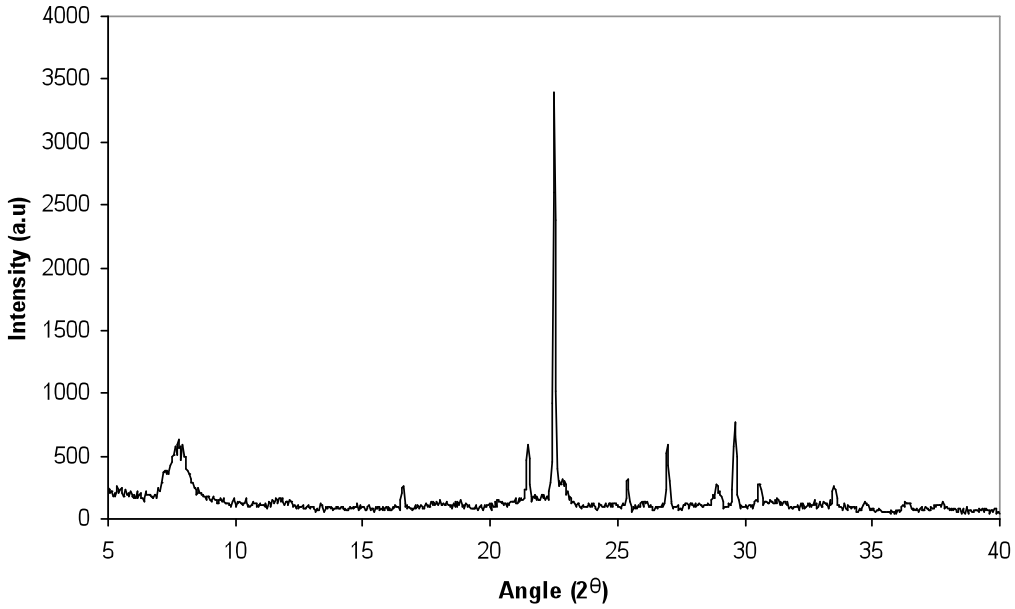

Fig. S4: Powder X-ray diffraction pattern of CH_3Sn-Beta

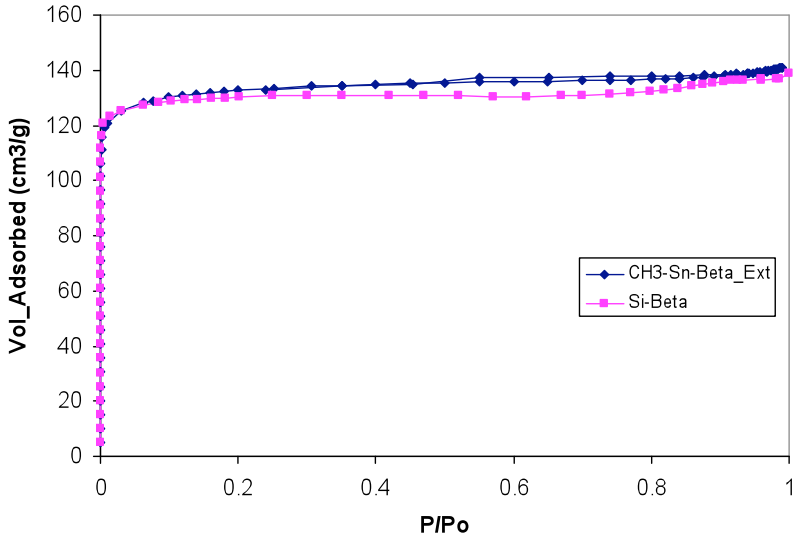

Fig. S5: N_2 adsorption isotherms of Si-Beta and CH_3Sn-Beta extracted.

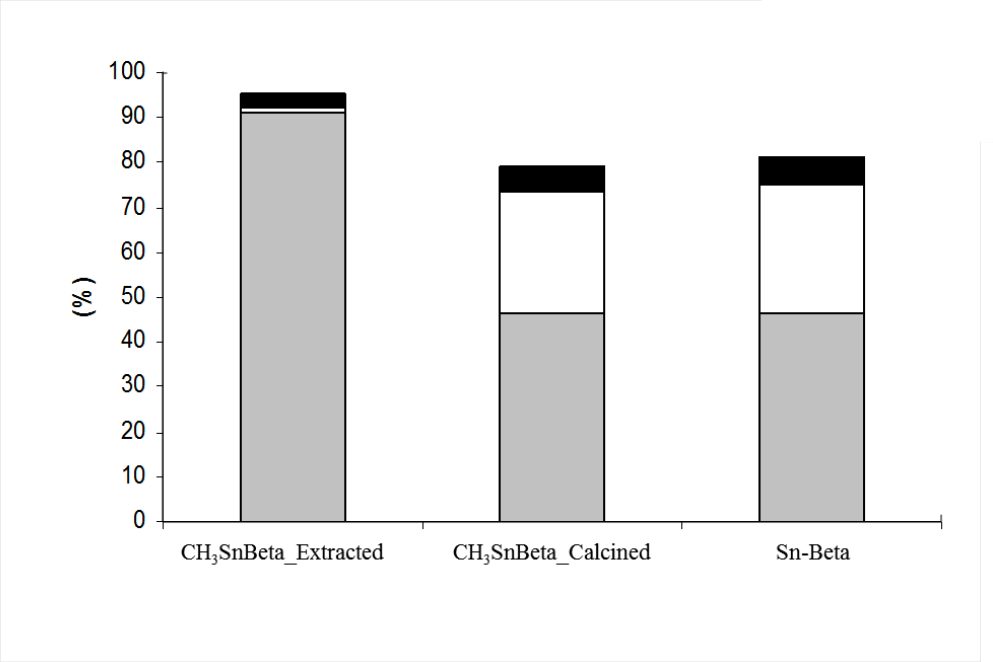

Fig. S6: Glucose isomerization reactivity with Sn-Beta and CH_3Sn-Beta. Grey: Glucose; White: Fructose; Black: Mannose. Reaction conditions: glucose:Sn = 100:1, 110 ^oC, 45 min.

Text S1 Calculation of the kinetic isotope effect.

The kinetic isotope effect is calculated using the expression shown below, derived from transition state theory. The difference in the rate constants between the activation of C-H and C-D bond results mainly for the difference in their zero-point energies (ZPE).

$$\frac{k_H}{k_D} = \exp\left(\frac{ZPE_H - ZPE_D}{kT}\right) = \exp\left(\frac{0.13*h*c*\overline{\nu}_H}{k*T}\right)$$

where $\frac{\overline{\nu}_D}{\overline{\nu}_H} \cong 0.74$, $ZPE = \frac{1}{2}h * c * \overline{\nu}$

h is the Planck's constant with the value of $6.63*10^{34}$ m^2kg/s, c is the speed of light with a value of $2.998*10^8$ m/s, $\overline{\nu}_H$ is the vibrational frequency or wavenumber of a C-H bond scissoring vibration with a value of ~1500 cm^{-1} (we have assumed that the shift of the proton from C2 of glucose to C1 of fructose goes through a bond scissoring vibration), k is the Boltzman constant with a value of $1.38*10^{-23}$ $m^2kg/s^2/K$ and T is the operating temperature in K.

Computational Studies

Text S2 Computational details

The computations in this paper were carried out using the B3LYP(*2*) and the MP2 levels of theory, which is similar to our previous work(*3*) where we reported a detailed mechanism for glyceraldehyde- dihydroxy acetone isomerization by a Sn-beta active site In the computations the Lewis acid metal atom is treated using CC-pVDZ-PP(*4*) , Ahlrich's VTZ(*5*) , 6-31+G(d) basis sets for Sn, Ti, and Si atoms, respectively. The 6-31+G(d) (BS1) basis set is used for the rest of the atoms. The B3LYP level of theory is used for geometry optimization. In order to assess dispersion energies and basis set superposition errors a single point energy evaluation is performed at the MP2 level of theory with a combination of aug-CC-pVQZ (BS2,for Sn(*4*),Ti(*6*),) and 6-311++G(3df,3pd) (rest of the atoms, BS3) on the geometry obtained from the density functional studies. Effective Core Potentials (ECP) for Sn, was used to include relativistic effects in both the DFT and MP2 calculations(*7*). Detailed benchmarking of the theory used in this paper against high level G4(*8*) and CCSD(T) levels of theory are described elsewere(*3*). Frequency calculations were performed to determine whether the stationary points are minima or transition states (TS) and to provide zero point energy corrections (ZPE). Free energy and enthalpy corrections at 298 K were also evaluated using the B3LYP level of theory. In order to account for the effects of aqueous environment, calculations were performed in water dielectric using the SMD solvation model(*9*) at the B3LYP level of theory with the same basis sets as used for the geometry evaluations. In order to evaluate the enthalpy of solvation the non-electrostatic contributions to the solvation energies were excluded. The calculations for this investigation were done using Gaussian 09(*10*)

Text S3: Isomerization catalyzed by Sn-Beta active site models

Information regarding the binding modes of glucose on the Sn-Beta active site is based on the affinity of keto group of the sugar molecule towards the Lewis acid sites and the active involvement of the hydroxyl group (Lewis base) in the open site, which acts as a Lewis base. It has been suggested that the actual active site of Sn-Beta is the $(SiO)_3Sn(OH)$ center and previous density functional studies were reported using this model to understand the energetics and mechanism of the Meerwein-Ponndroff-Verley-Oppenauer reactions (MPVO) between cyclohexanone and 2-butanol(*11*). A recent density functional study also provided insight into the possible role of hydrolyzed T-9 active site of Sn-Beta (Scheme S1 (a) in catalyzing the hydride-shift during the isomerization of aldose to ketose.

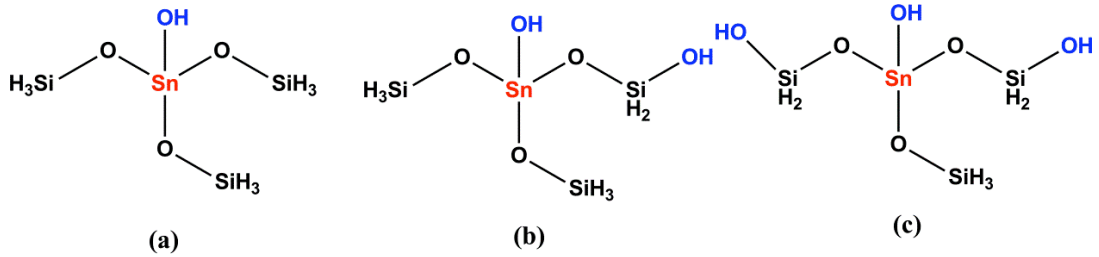

Scheme S1: Schematic representation of the T-9 site of Sn-Beta models used in the computational study: (a) hydrolyzed model, (b) hydrolyzed model with an adjacent single silanol group; and (c) hydrolyzed model with two silanol groups

In aqueous media, the solvation effects of glucose are relatively larger compared to that of a confined space such as in a zeolite pore. In addition to the solvent effect, binding of glucose would be also be affected by the dispersive interaction from the zeolite pore. Therefore, we have incorporated the solvation effect throughout the calculations for determining the free energy and enthalpy profile, and used MP2 level calculations. Thermodynamically, the most favorable binding is through a ring oxygen and an adjacent hydroxyl oxygen ion (C_1-OH, after deprotonation) coordinates to the metal center in aqueous environments. This model provides insight to the reaction barrier for the ring opening mechanism with the participation of basic hydroxyl group in the presence of the central metal atom. An alternative binding mode of glucose would be through its hydroxyl groups to the metal center; however, the free energy of this interaction is thermodynamically uphill both in gas phase and in aqueous environment. Binding through the ring oxygen and the hydroxyl group at C1 position was computed as thermodynamically more favorable compared to any two hydroxyl groups of glucose. Therefore, this was considered as the initial binding mode of glucose to the active site in this study. From this binding mode, we have proposed a mechanism, which involves the ring opening, hydride shift, ring closing and computed a detailed free energy profile at the MP2 levels of theory in a water dielectric (298 K) for the conversion of glucose to fructose by the Sn-active site model. The computed free energy profile is shown in Figure S7 and the enthalpy profile is shown Figure S8. All energies are relative to the initial state **A**, the sum of the isolated Sn-$(OSiH_3)_3$-OH active site and glucose in aqueous dielectric at infinite distance. The interaction of cyclic glucose with the active site model (Scheme S1, (a)) to form the initial complex (**I**) is thermodynamically downhill and highly exothermic (-17.1 kcal/mol) in aqueous media. The Gibbs free energy of complexation is quantitatively smaller than the change in enthalpy in solution due to the decrease in entropy upon binding to the active site. Additionally, the free energy of complexation in solution is quantitatively smaller than the gas phase due to the decrease in solvation energy of hydrophilic glucose upon complexation. The hydroxyl group (Lewis base) of the active site picks up a proton from the C_1-OH and forms a water molecule and an open chain aldehyde (II). This process (proton transfer) requires a Gibbs free energy barrier of 10.6 kcal/mol (3.3 kcal/mol in gas phase) and results in the formation of a strong Sn-O_{ring} bond of 2.04 Å and weak Sn----OH_2(2.33 Å) bond. The cleavage of the Sn-O_{ring} bond occurs through the protonation of oxygen by the water ligand resulting in the formation of acyclic glucose weakly coordinated with the catalytic center (III).

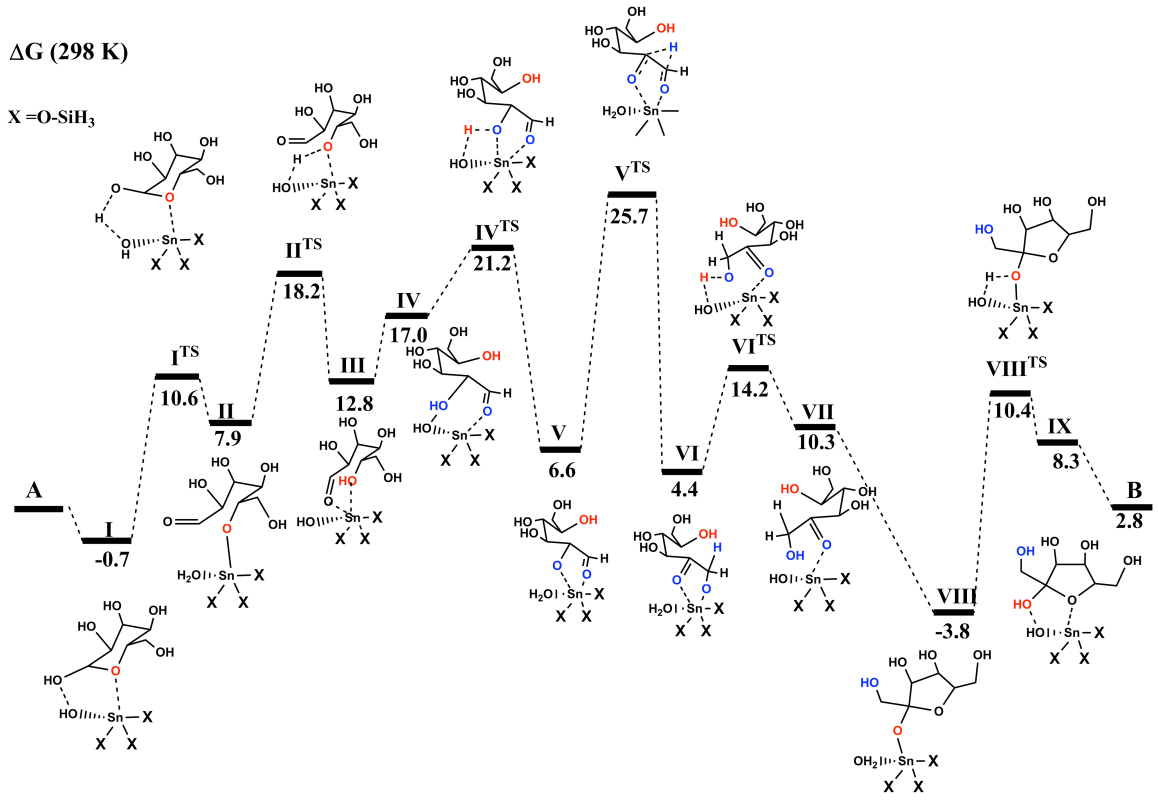

Fig. S7: The computed Gibbs free energy landscape of the isomerization of glucose-fructose catalyzed by the Sn-$(OSiH_3)_3$-OH active site model at the MP2 level of theory in an aqueous dielectric medium. The aqueous effects were modeled using the SMD solvation model at 298 K. The label A denotes the sum of Gibbs free energy of glucose and active site model (a) (Scheme 1) infinitely separated in aqueous medium, the B denotes the same quantity for fructose. All energies are in kcal/mol.

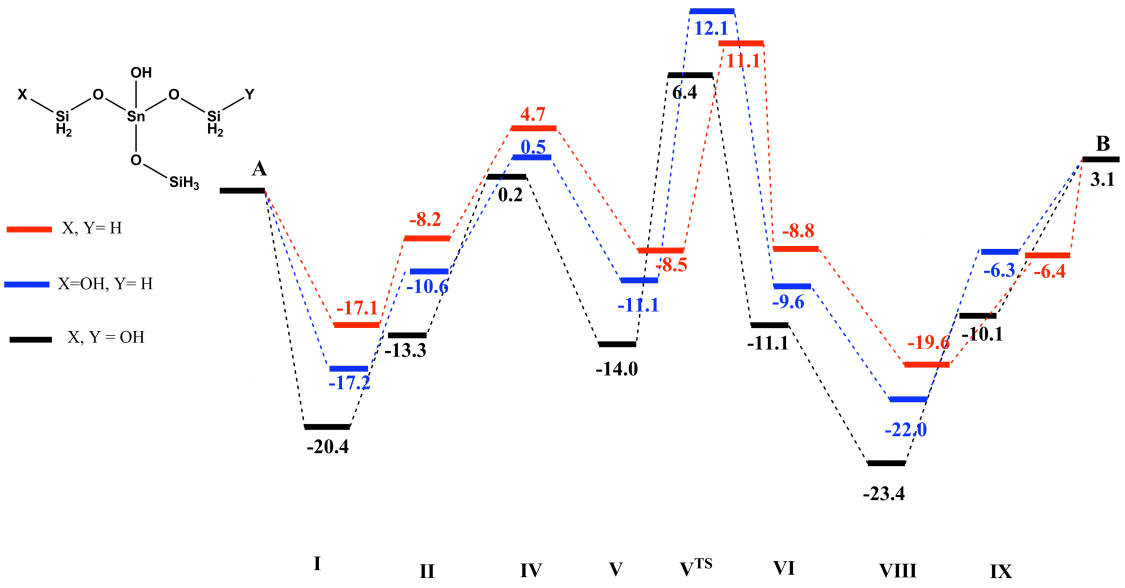

Fig. S8: The computed enthalpy profile (MP2, at 298 K in water dielectric) for glucose-fructose isomerization catalyzed by different open sites of Sn-Beta. The reaction coordinates are given in the X-axis. The label A denotes the sum of enthalpy of glucose and active site models infinitely separated in aqueous medium, B denotes the same quantity for fructose. All energies are relative to the energy of A and reported in kcal/mol.

This process requires an activation free energy of 18.2 kcal/mol (II^{TS}) and this process (II to III) of partially detaching acyclic glucose from the active site is thermodynamically uphill (4.9 kcal/mol). Binding of acyclic glucose to the Sn-active site is much weaker than cyclic glucose and moderately uphill compared to the free energy of the initial state **A** in aqueous solution. Deprotonation of the hydroxyl group at the C_2 position by the Lewis base requires an apparent activation free energy barrier of 21.2 kcal/mol and the computed true barrier ($IV \rightarrow IV^{TS}$) for this proton transfer is 4.2 kcal/mol. This process (IV to V) is thermodynamically downhill (by 11.0 kcal/mol) due to formation of a Sn-O bond and water. This process is followed by the hydride shift from the C2 to C1 carbon atom (**V** to **VI**). The hydride shift occurs through a hexa-membered transition state and requires an apparent activation free energy barrier of 25.7 kcal/mol with the active participation of a tin atom by activation of the keto oxygen atoms of the sugar molecule. The true activation free energy barrier for ($V \rightarrow V^{TS}$) is 19.1 kcal/mol and the true activation enthalpic barrier for this reaction is 19.6 kcal/mol. Also note that, the apparent activation enthalpy barrier for this reaction is 11.1 kcal/mol in aqueous solution and the hydride shift (V→VI) is a thermodynamically downhill process. The hydride shift is followed by the transfer of a proton from the water ligand to the oxygen attached to the C1 carbon (VI to VII) and then ring closure (VII to VIII). The first process occurs through the deprotonation of a water ligand and the resulting hydroxyl group transforms back to water through re-protonation from the hydroxyl group attached to the C_6 carbon atom. The activation free energy barrier for the reaction VI to VII is 14.2 kcal/mol. The ring closure ($VIII^{TS}$) from the intermediate (VIII) is calculated to be barrier-less in aqueous solution due to the relative stabilization from aqueous dielectric for the cyclic fructo-furanose form. The complex formed (VIII) after the ring closure is

thermodynamically stable and has a relative free energy of -3.8 kcal/mol in aqueous solution. A proton transfer (activation free energy barrier of 10.4 kcal/mol) from water ligand to the oxygen atom cleaves the Sn-O bond forming, the intermediate IX. This intermediate is 8.3 kcal/mol higher in free energy than **A**. The separated cyclic fructose and the active site model (B) that form from IX have an energy of 2.8 kcal/mol relative to A. The highest point in the free energy profile is the hydride shift, which is assumed to be the rate-limiting step. This is consistent with the recently published experimental studies(*12, 13*)

Text S4 Calculation of Apparent activation enthalpy

The apparent enthalpy was obtained by performing a micro-kinetic analysis using the elementary steps in enthalpy profiles (Sn-Beta: Figure S8, Ti-Beta : Figure S10, vide infra) for each of the active sites. The 1,2-hydride shift was assumed to be the rate limiting step. The apparent activation enthalpy can be calculated using the following equation,

$$H_{apparent}^{act} = H_{true}^{act} + \Delta H^{adsorption},$$

where $H_{apparent}^{act}$, H_{true}^{act}, and $\Delta H^{adsorption}$ are apparent activation enthalpy, true barrier (hydride shift), and change in enthalpy of adsorption of the most abundant intermediates (exothermic adsorption), respectively.

The $\Delta H^{adsorption} = \Sigma \Delta H^{reactant\ intermediates} - \Sigma \Delta H^{product\ intermediates}$. Using the above expression, the apparent activation enthalpies for the glucose-fructose isomerization catalyzed by Sn-Beta active site models (a, b, c in Scheme S1) were computed and shown in Table S1.

Table S1: Computed true activation enthalpy (H^{act}_{true}), change in adsorption enthalpy ($\Delta H^{adsorption}$) and apparent enthalpy of activation ($H^{act}_{apparent}$) for glucose-fructose isomerization catalyzed by active site models for Sn-Beta (Scheme S1: a, b, c) and Ti (Scheme S2: d, e, f). The energy evaluated at the MP2 level of theory. The calculations are performed at 298 K, and contribution to enthalpies from aqueous dielectric is also included. All energies are reported in kcal/mol**.**

active site model	H^{act}_{true}	$\Delta H^{adsorption}$	$H^{act}_{apparent}$
(a)	19.6	-1.0	18.6
(b)	23.2	-1.1	22.1
(c)	20.6	-3.3	17.3
(d)	20.2	+7.8	28.0
(e)	20.2	+14.1	34.3
(f)	17.6	+18.8	36.4

The computed activation enthalpies for glucose to fructose isomerization catalyzed by active site models a, b, and c (Scheme S1) are 18.6, 22.1, and 17.3 kcal/mol respectively. The computed activation enthalpy of active site model b (22.1 kcal/mol), Sn-Beta active site with one adjacent Si-OH group is consistent with the experimental activation energy of 21.2 kcal/mol from our experimental kinetic studies. These results suggest that the active site for the Sn Beta, which promotes the isomerization process, is in fact a hydrolyzed site rather than the close site. Previously it was shown that, the apparent activation energy for the hydride shift associated with the isomerization of glyceraldehyde to dihydroxy acetone is 10 kcal/mol higher for the closed site than the open site.(*3*)

Text S5 Isomerization catalyzed by Sn-Beta Closed Site model.

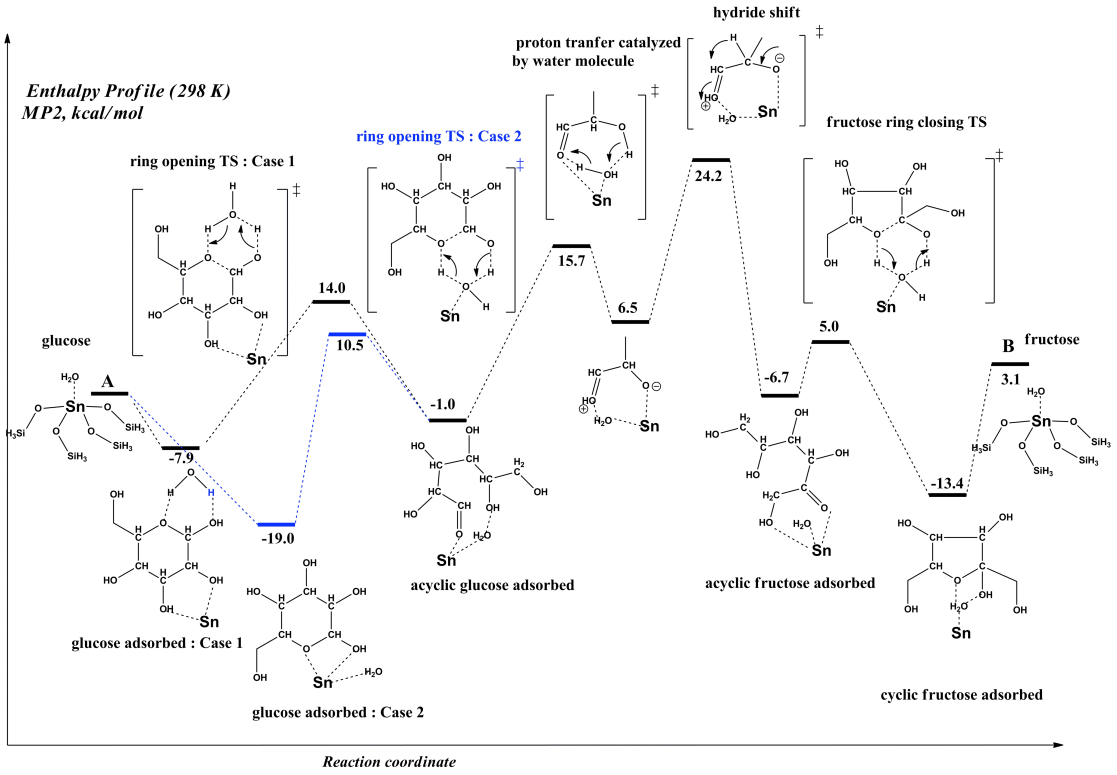

Fig. S9: The computed enthalpy profile of the isomerization of glucose-fructose catalyzed by the Sn-$(OSiH_3)_4$- H_2O active site model at the MP2 level of theory in an aqueous dielectric medium. The aqueous effects were modeled using the SMD solvation model at 298 K. The label A denotes the sum of Gibbs free energy of glucose and active site model (Sn-$(OSiH_3)_4$- H_2O) infinitely separated in aqueous medium, the B denotes the same quantity for fructose. All energies are reported in kcal/mol**.**

The detailed enthalpy profile for the glucose-fructose isomerization catalyzed by Sn-Beta closed site (**Sn-$(OSiH_3)_4$- H_2O)** is shown in Figure S9. Due to the lack of a Lewis base in the closed site model the ring opening and closure is catalyzed by water which is coordinated with Sn site. Different modes of cyclic glucose adsorption were considered. Our calculations suggest that upon strong adsorption of glucose (Case 2 in Figure S9), the rate-limiting step is the ring opening of glucose, while for weaker absorption the rate-limiting step is the hydride shift. Based on the micro-kinetic model, the computed apparent activation enthalpy is 30 kcal/mol regardless of the initial adsorption. These calculations suggest that the closed site can also catalyze the isomerization process, but not a primary catalytic site due to requirement of a relatively larger activation enthalpy compared to the open site. Another important observation is the relative stability of complex formed upon adsorption of acyclic fructose with closed site compared to open site.

Text S6 Isomerization catalyzed by Ti-Beta active site models

We have also utilized MP2 theory to calculate the energy associated with elementary steps involved in the isomerization of acyclic glucose to fructose on a number of different Ti-Beta active site models including: (d) an open site where framework Ti is bound in one direction with an OH group and in the other three directions with framework Si through bridging oxygen atoms , (e) an open site as in (f) with an one adjacent silanol (Si-OH) group, and an open site as in (d) with two adjacent silanol (Si-OH) groups (Scheme S2) We found that the lowest energy pathway for the isomerization of acyclic glucose to fructose on all the Ti-Beta active sites involves a hydride shift from the second carbon (C2) in acyclic glucose to the first carbon (C1) in fructose as the rate-limiting step, similar to open site of Sn-Beta (Figure S7). Here, we have computed the detailed enthalpy profile for glucose-fructose isomerization catalyzed by all these sites (Figures S9 and S10) for comparison with the experiments and with the Sn-Beta results.

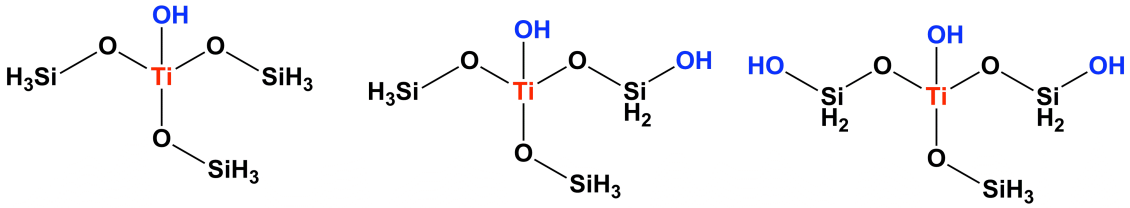

Scheme S2: Schematic of different Ti-Beta active sites used in the computational models. d) open Ti site, e) open Ti site with one Si-OH group and f) open Ti site with two Si-OH group**.**

Figure S10 presents a comparison of the enthalpy profile for the glucose-fructose isomerization by open site of Sn-Beta (with one silanol) and Ti-Beta (with one silanol group). The computed rate limiting step and the initial enthalpy of binding of glucose suggests that Sn-Beta is a much superior catalyst for the isomerization than the Ti-Beta. This is consistent with the reported studies. Figure S11 shows the calculated energetics (enthalpies) associated with various elementary steps involved in the isomerization of acyclic glucose to fructose on the three different active sites. We found that for all three models of the active site (d, e, f), the rate limiting step is the 1,2 hydride shift. The computed apparent activation energies for glucose-fructose isomerization catalyzed by Ti-Beta active site models (d,e,f) is given in Table S1.

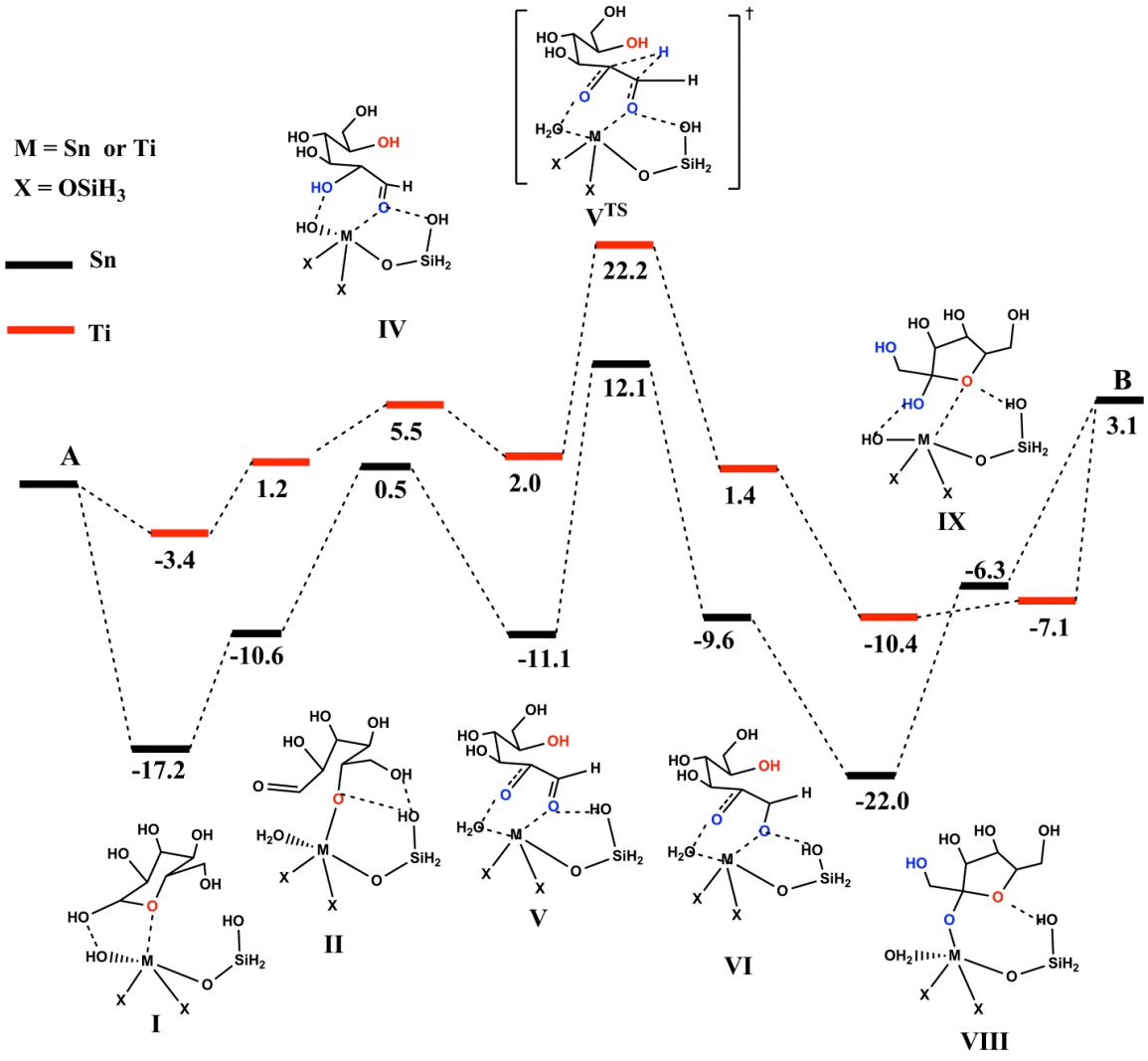

Fig. S10: Comparison of the enthalpic profile of the open site of Sn-Beta and Ti-Beta for the glucose-fructose isomerization. The MP2 level of theory is employed to compute the enthalpy surface. The solvation contribution in the enthalpy is computed using the SMD solvation model. The label A denotes the sum of enthalpy of glucose and active site model (b and e) infinitely separated in aqueous medium, the B denotes the same quantity for fructose. All energies are reported in kcal/mol.

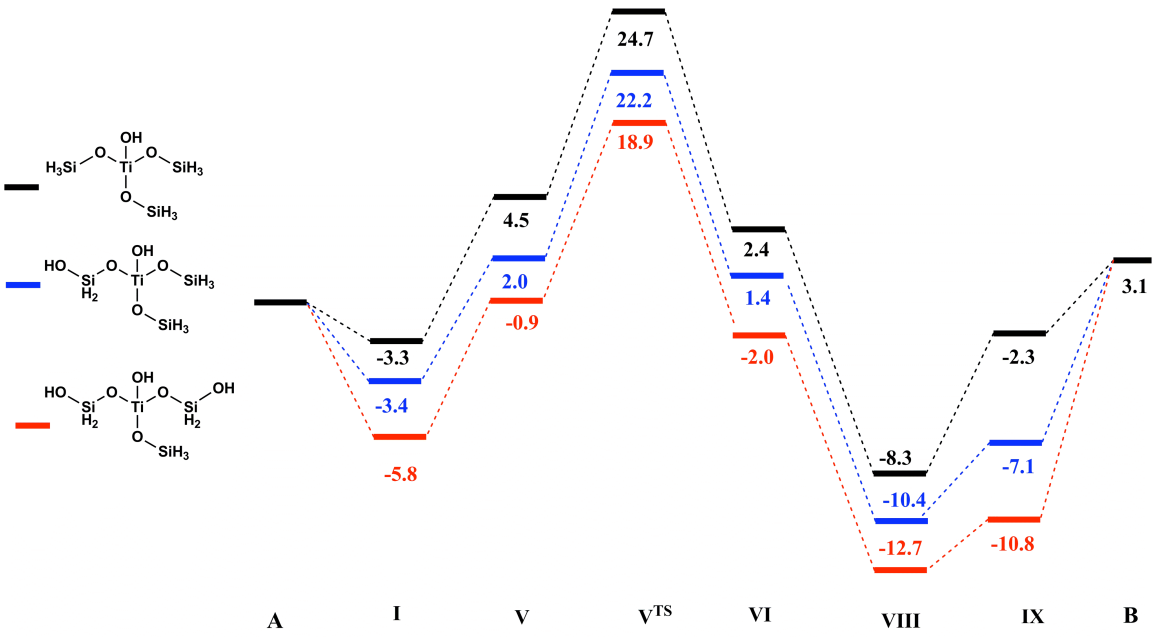

Fig. S11: Enthalpy profile (MP2) for the glucose-fructose isomerization by different Ti-Beta active site models. The X-axis denotes the reaction coordinate. See Figure S9 for the schematic representation for species II to IX. The label A denotes the sum of enthalpy of glucose and active site model (d,e,f) infinitely separated in aqueous medium, the B denotes the same quantity for fructose. All energies are reported in kcal/mol.

The computed apparent enthalpy for the glucose-fructose isomerization catalyzed by models d, e, and f (Scheme S2) are 28.0, 34.3 and 36.3 kcal/mol respectively. If we compare our calculated overall activation barriers with the measured barriers we find that our measured activation enthalpy (37.1 kcal/mol) is very similar to the one calculated for the Ti open site with one and two silanol group model system (34.3 & 36.3 kcal/mol). Since the apparent activation barriers for the open Ti site with one and two adjacent silanol group are very close in energy, it would be difficult to distinguish between these two sites based on the MP2 calculations. Therefore, we can only conclude based on comparing the MP2 calculations with the experimental data that the active site in Ti-Beta is a form of an open Ti site, which involves a hydrated Ti-OH center with adjacent silanol groups.

References:

1. M. Tamarasso, G. Perego, B. Notari. (U.S Pat. 4,410,501, 1983).
2. A. D. Becke, Density-Functional Thermochemistry .3. The Role of Exact Exchange. *J. Chem. Phys.* **98**, 5648 (1993).
3. R. S. Assary, L. A. Curtiss, Theoretical Study of 1,2-Hydride Shift Associated with the Isomerization of Glyceraldehyde to Dihydroxy Acetone by Lewis Acid Active Site Models. *J. Phys. Chem. A* **115**, 8754 (2011).

4. K. A. Peterson, Systematically convergent basis sets with relativistic pseudopotentials. I. Correlation consistent basis sets for the post-d group 13-15 elements. *J. Chem. Phys.* **119**, 11099 (2003).
5. A. Schafer, H. Horn, R. Ahlrichs, Fully Optimized Contracted Gaussian-Basis Sets for Atoms Li to Kr. *J. Chem. Phys.* **97**, 2571 (1992).
6. N. B. Balabanov, K. A. Peterson, Systematically convergent basis sets for transition metals. I. All-electron correlation consistent basis sets for the 3d elements Sc-Zn. *J. Chem. Phys.* **123**, (2005).
7. P. J. Hay, W. R. Wadt, Abinitio Effective Core Potentials for Molecular Calculations - Potentials for the Transition-Metal Atoms Sc to Hg. *J. Chem. Phys.* **82**, 270 (1985).
8. L. A. Curtiss, P. C. Redfern, K. Raghavachari, Gaussian-4 theory. *J. Chem. Phys.* **126**, 084108 (2007).
9. A. V. Marenich, C. J. Cramer, D. G. Truhlar, Universal Solvation Model Based on Solute Electron Density and on a Continuum Model of the Solvent Defined by the Bulk Dielectric Constant and Atomic Surface Tensions. *J. Phys. Chem. B* **113**, 6378 (2009).
10. Gaussian 09, M. J. Frisch, G. W. Trucks, H. B. Schlegel, G. E. Scuseria, M. A. Robb, J. R. Cheeseman, G. Scalmani, V. Barone, B. Mennucci, G. A. Petersson, H. Nakatsuji, M. Caricato, X. Li, H. P. Hratchian, A. F. Izmaylov, J. Bloino, G. Zheng, J. L. Sonnenberg, M. Hada, M. Ehara, K. Toyota, R. Fukuda, J. Hasegawa, M. Ishida, T. Nakajima, Y. Honda, O. Kitao, H. Nakai, T. Vreven, J. A. Montgomery, Jr., J. E. Peralta, F. Ogliaro, M. Bearpark, J. J. Heyd, E. Brothers, K. N. Kudin, V. N. Staroverov, R. Kobayashi, J. Normand, K. Raghavachari, A. Rendell, J. C. Burant, S. S. Iyengar, J. Tomasi, M. Cossi, N. Rega, J. M. Millam, M. Klene, J. E. Knox, J. B. Cross, V. Bakken, C. Adamo, J. Jaramillo, R. Gomperts, R. E. Stratmann, O. Yazyev, A. J. Austin, R. Cammi, C. Pomelli, J. W. Ochterski, R. L. Martin, K. Morokuma, V. G. Zakrzewski, G. A. Voth, P. Salvador, J. J. Dannenberg, S. Dapprich, A. D. Daniels, Ö. Farkas, J. B. Foresman, J. V. Ortiz, J. Cioslowski, and D. J. Fox, Gaussian, Inc., Wallingford CT, 2009.
11. M. Boronat, A. Corma, M. Renz, Mechanism of the Meerwein-Ponndorf-Verley-Oppenauer (MPVO) Redox Equilibrium on Sn- and Z-Beta Zeolite Catalysts. *J. Phys. Chem. B* **110**, 21168 (2006).
12. M. Moliner, Y. Román-Leshkov, M. E. Davis, Tin-containing zeolites are highly active catalysts for the isomerization of glucose in water. *Proc. Nat. Acad. Sci.* **107**, 6164 (2010).
13. Y. Román-Leshkov, M. Moliner, J. A. Labinger, M. E. Davis, Mechanism of Glucose Isomerization Using a Solid Lewis Acid Catalyst in Water. *Angew. Chem. Int. Ed.* **49**, 8954 (2010).